Biochemistry

 Volume 40, Number 42 October 23, 2001

Accelerated Publications

Evidence for DNA Charge Transport in the Nucleus†

Megan E. Núñez,‡ Gerald P. Holmquist,§ and Jacqueline K. Barton*,‡

Division of Chemistry and Chemical Engineering, California Institute of Technology, Pasadena, California 91125, and Beckman Research Institute, City of Hope Cancer Center, Duarte, California 91010

Received July 26, 2001

ABSTRACT: Oxidative damage to DNA bases in isolated *HeLa* nuclei occurs upon treatment with rhodium intercalators and photoactivation. Oxidation occurs preferentially at the 5′-guanine of 5′-GG-3′ sites, indicative of base damage by DNA-mediated charge transfer chemistry. Moreover, oxidative damage occurs at protein-bound sites which are inaccessible to rhodium. Thus, on transcriptionally active DNA within the cell nucleus, DNA-mediated charge transport leads to base damage from a distance, and direct interaction of an oxidant is not necessary to generate a base lesion at a specific site. These observations require consideration in designing new chemotherapeutics and in understanding cellular mechanisms for DNA damage and repair.

DNA inside of cells can be damaged by a variety of agents to generate unnatural and potentially mutagenic base lesions (*1*). Modified or functionalized bases can be induced by direct ionization by high-energy X-ray and γ-ray sources, irradiation with UV light, interactions with reactive oxygen species, and reactions with a diverse set of small molecules, both therapeutic and carcinogenic. Studies of DNA-mediated charge transport have elucidated another possible mechanism for the generation of base lesions (*2*, *3*). A variety of methods have demonstrated that the stacked aromatic base pairs of DNA provide an efficient medium for charge transport, including oxidation of bases from a distance through the base pair stack (*4*, *5*). A metallointercalator covalently tethered to one terminus of an oligodeoxynucleotide duplex can oxidize 5′-GG-3′ sequences up to 200 Å away (*6*, *7*). The efficiency of this long-range oxidation displays a very weak dependence on distance, but it is sensitive to coupling of the oxidant into the base pair stack and to the stacking of the intervening base pairs (*4*, *8*−*10*). Because of their well-characterized binding and photochemical properties, rhodium(III) complexes were first utilized to study oxidative DNA damage from a distance, but long-range oxidative damage has now been demonstrated using a variety of photooxidants, indicating that this reaction is characteristic of the DNA itself and is not a property of an unusual photooxidant. Photoactivation of naphthalimides, Ru(III) intercalators, ethidium, anthraquinones, and even sugar radicals has been shown to promote oxidative damage to 5′-GG-3′ sites from a distance (*11*−*16*).

To examine whether charge migration through DNA occurs within the cell, isolated whole nuclei were incubated with a rhodium intercalator, $Rh(phi)_2DMB^{3+}$, and then irradiated with ultraviolet light above ~320 nm. Phenanthrenequinone diimine (phi)[1] complexes of rhodium bind to DNA avidly from the major groove by intercalation of the phi ligand into the base pair stack (*17*) (Figure 1a). These

† This work was supported by a grant from the NIH (GM49216) as well as funding from the National Foundation for Cancer Research and the Howard Hughes Medical Institute predoctoral fellowship program (M.E.N.).

* To whom correspondence should be addressed. E-mail: jkbarton@caltech.edu.

‡ California Institute of Technology.

§ City of Hope Cancer Center.

[1] Abbreviations: phi, phenanthrenequinone diimine; DMB, 4,4′-dimethyl-2,2′-bipyridine; LMPCR, ligation-mediated PCR; PGK, phosphoglycerate kinase.

10.1021/bi011560t CCC: $20.00
Published on Web 09/27/2001

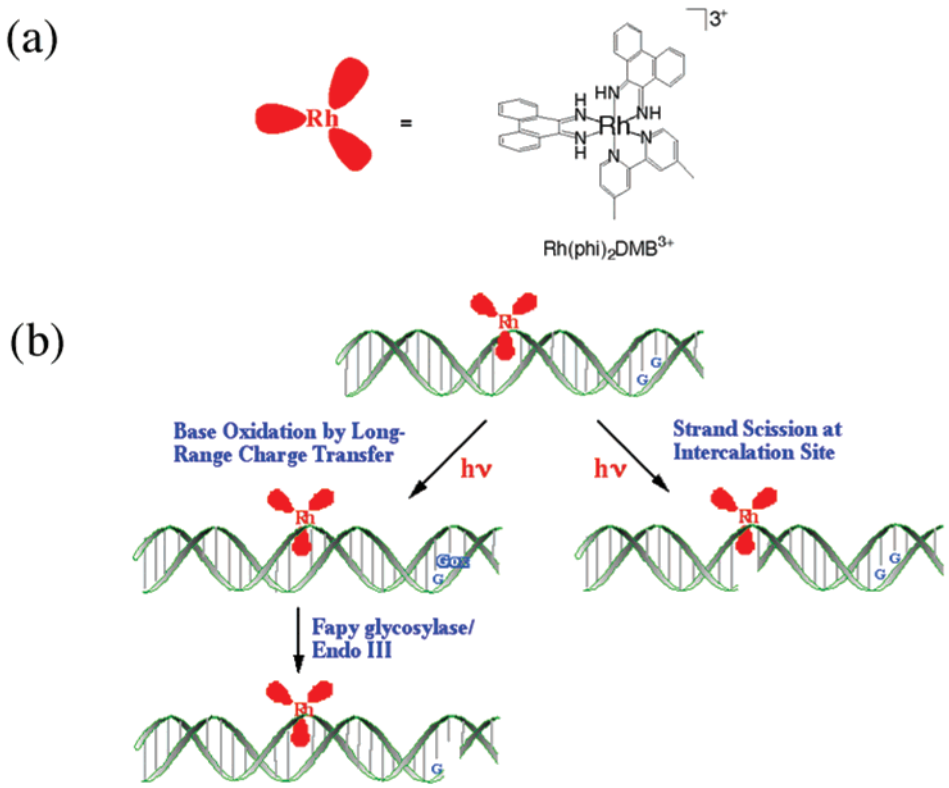

FIGURE 1: Photoreactions of the rhodium complexes with DNA. (a) Structure of the rhodium complex $Rh(phi)_2DMB^{3+}$. When phi complexes of rhodium bind to DNA, one of the phi ligands intercalates into the DNA and the other two ancillary ligands lie along the major groove (*17*). (b) Mechanisms of DNA photocleavage by $Rh(phi)_2DMB^{3+}$. Upon photoexcitation with near-ultraviolet light, the complex oxidizes the 5′-guanine of 5′-GG-3′ sites from a distance by long-range charge transfer through the DNA base pair stack. The damaged guanine bases that result from this oxidation are revealed by treatment with the base excision repair enzymes formamidopyrimidine DNA glycosylase and endonuclease III (Fapy glycosylase and EndoIII, respectively). When the rhodium complex is photoexcited at higher energy, the sugar−phosphate backbone is cleaved directly at the site of intercalation. These frank strand breaks do not require enzyme treatment to be revealed. When the metal complex is irradiated with both wavelengths of light simultaneously, a combination of products results. It is then possible to determine which bases are oxidized by looking at the difference between the cleavage events in the absence of Fapy glycosylase and EndoIII (frank strand breaks) and in the presence of Fapy glycosylase and EndoIII (base oxidation chemistry with frank strand breaks).

complexes react with DNA according to two distinct mechanisms when irradiated between 300 and 400 nm (Figure 1b). They generate a frank strand break at the intercalation site, giving products consistent with the abstraction of the 3′-hydrogen of the sugar by the metal complex (3′- or 5′-phosphates, free bases, base propenoic acids, and 3′-phosphoglycaldehydes) (*18*). Since this reaction does not involve a diffusible intermediate, it can be used to determine precisely where the metal complex is bound. Phi complexes of rhodium can also oxidize guanine bases through a long-range reaction that is mediated by the DNA π stack (*3*, *4*). The oxidized guanine radical intermediates are trapped by oxygen or water to form a variety of irreversible products, including 8-oxoguanine, formamidopyrimidine, oxazalone, and imidazalone derivatives (*19*). These modified base products do not generally disrupt the sugar−phosphate backbone, but they can be converted to strand breaks with 5′-phosphate termini by subsequent treatment with a mixture of the base-excision repair enzymes endonuclease III (EndoIII) and formamidopyrimidine DNA glycosylase (Fapy glycosylase). The hydrogen abstraction and long-range oxidation reactions can be isolated by excitation with specific wavelengths of light. However, when the metal complex is irradiated with both wavelengths of light simultaneously, as we have done here, a combination of products results. It is then possible to determine which bases are oxidized by looking at the difference between the cleavage events in the absence of Fapy glycosylase and EndoIII (frank strand breaks) and presence of Fapy glycosylase and EndoIII (base oxidation chemistry with frank strand breaks).

Preferential oxidation of 5′-guanines of 5′-GG-3′ doublets and other guanine multiplets is the characteristic signature of charge transfer through the DNA base stack, whereas oxidation of all guanines equally or reaction of other bases points to a different mechanism of damage (*3*, *19*). Guanine bases are oxidized preferentially because they have the lowest oxidation potential of the four canonical nucleotide bases (*20*), and a selectivity for 5′-guanines of 5′-GG-3′ sites arises from the effects of base stacking on the ionization potentials of the bases (*21*, *22*). Oxidation potentials increase in the following order: 5′-GGG-3′ < 5′-GG-3′ < 5′-GA-3′ ≪ 5′-GC-3′ and 5′-GT-3′.

Here we examine oxidative damage to DNA within the nucleus by photoactivation of nuclei containing $Rh(phi)_2DMB^{3+}$. Ligation-mediated PCR (LMPCR) can be used to assess the pattern of base damage for genes of interest (*23*), and to establish whether oxidative damage to the DNA may occur at sites spatially separated from the photooxidant.

MATERIALS AND METHODS

Nuclear Isolation and Photoirradiation with the Rhodium Metallointercalator. Nuclei and genomic DNA were isolated

from *HeLa* cells according to the method of Pfeifer and Riggs (*24*). Nuclei were isolated by a 5 min lysis in cold buffer A+ [0.3 M sucrose, 60 mM KCl, 15 mM NaCl, 60 mM Tris-HCl (pH 8), 0.5 mM spermidine, 0.15 mM spermine, 2 mM EDTA, and 0.5% Nonidet], followed by centrifugation to pellet nuclei. The nuclei were then resuspended in this buffer with 33 μM $Rh(phi)_2DMB^{3+}$ and immediately photoirradiated on ice for 1 h using an Oriel 1000 W UV solar simulator and a 360 nm cutoff filter. Whole *HeLa* cells were also incubated with the rhodium complex and photoirradiated, but a stronger signal was observed for DNA isolated from rhodium-treated nuclei. After isolation from nuclei, untreated naked genomic DNA was suspended in TE to a concentration of ~100 μg/mL with 33 μM Rh and photoirradiated for 1 h without preincubation. Control samples of whole cells, nuclei, or naked genomic DNA that lacked either Rh or photoirradiation were also prepared. Polyamines were generally used in the nuclear isolation buffer to maintain the ionic strength. Photoirradiation of identical samples lacking polyamines showed that although the presence of polyamines does not affect the general pattern of protein footprints as measured using photoexcited rhodium complexes, they do enhance the oxidation of guanine bases relative to frank strand breaks. Control reactions lacking rhodium demonstrated that the polyamines do not themselves oxidize or cleave DNA.

LMPCR and Data Analysis. After isolation and purification, the DNA was treated with a mixture of Fapy DNA glycosylase and endonuclease III where applicable, which removes a variety of modified base lesions and breaks the DNA backbone, generating 5′-phosphate termini (*25*). Aliquots (1 μg) of DNA and Maxam−Gilbert sequencing standards were amplified by LMPCR manually using *Pfu* Turbo polymerase from Stratagene (La Jolla, CA) and primer sequences and reaction mixtures as described previously (*26*). Ligation-mediated PCR involves first a primer-extension step followed by ligation of a linker to the blunt ends of the DNA (*23*). PCR is then carried out using primers to the gene of choice on one end and to the linker on the other. A series of nested primers are used for these steps to increase the specificity of the amplification for the gene of choice. The rhodium hydrogen abstraction reaction generates a variety of frank strand breaks with different termini (*18*); however, only 5′-phosphate termini are amplified by the LMPCR reaction, so some of the $Rh(phi)_2DMB^{3+}$ frank break sites may not be amplified.

The LMPCR products were separated and visualized by denaturing polyacrylamide gel electrophoresis using a LI-COR DNA model 4200 automated sequencer (LI-COR, Inc., Lincoln, NE) and were analyzed using the "RFLP Scan" program (Scanalytics, Inc., Fairfax, VA). Data sets were normalized if necessary to account for uneven gel loading by multiplying each measurement in one lane uniformly by a constant such that the total intensity of each lane (sum of all of the band intensities) was the same. No bands appeared in the control lanes in the p53 region. PCR amplification of the PGK region showed four bands above background that were deleted from all data sets.

Because the products of the cleavage reactions are amplified through a series of LMPCR steps, it is generally not feasible to combine the results of multiple manual experiments directly to obtain error bars (however, see ref *26*). As a result, each of the histograms shown in this paper illustrates the data from a single experiment. However, all of the experiments were repeated multiple times, both from the LMPCR step forward and from the first DNA isolation and nuclear irradiation steps using new batches of *HeLa* cells, to ensure that the patterns of frank strand breaks and base oxidation are reproducible.

RESULTS AND DISCUSSION

Oxidative Damage within the p53 Gene. The damage induced by $Rh(phi)_2DMB^{3+}$ and near-ultraviolet light in nuclear DNA was monitored first on exon 5 of the p53 gene. Some frank strand breaks are present across the exon, indicating that the rhodium complex intercalates throughout the DNA (Figure 2a). As published previously, although the complex shows no high site specificity, there is a minor preference for the pyrimidine-containing strand of a base pair (*18*, *27*, *28*). Treatment with the mixture of base excision repair enzymes Fapy glycosylase and EndoIII causes new bands to appear. The difference between DNA samples before and after treatment with Fapy glycosylase and EndoIII represents the base specific damage (Figure 2b). The most heavily damaged positions are the 5′-GGG-3′ trinucleotide and the 5′-GG-3′ dinucleotides, followed in intensity by 5′-GA-3′ dinucleotides, which follows the order of their oxidation potentials. This pattern is fully consistent with electron transfer damage. In addition, base damage occurs preferentially at the 5′-guanines of the these sites rather than at the 3′-guanines or -adenines. A 5′-bias is characteristic of charge transfer damage but inconsistent with damage by singlet oxygen or other reactive oxygen species (*19*, *22*). The damage seen at guanine doublets and multiplets is not caused by the light source or any component of the buffer, as both frank strand breaks and oxidized bases are absent in the absence of rhodium.

Oxidative Damage within a Transcriptionally Active Promoter. Though the DNA damage generated inside of nuclei occurs at 5′-GG-3′ sites, consistent with a DNA charge transfer reaction, these data do not firmly establish that base oxidation occurs from a distance inside of nuclei. To explore this possibility, we examined a promoter region where rhodium binding should be selectively inhibited by the presence of transcription factors bound to the DNA (Figure 3). If guanine doublets are oxidized at these sites where the rhodium complex cannot bind directly, then oxidative damage must occur by a long-range mechanism. Furthermore, the dual nature of the rhodium photochemistry can be used to demonstrate directly that intercalation and oxidation occur at spatially distinct sites. Direct backbone scission by phi complexes of rhodium has been used to footprint restriction enzymes and even distamycin, a small minor groove-binding molecule, on restriction fragments (*28*). Conversely, long-range oxidation has been shown to occur through protein binding sites if the proteins do not disturb the DNA base stack (*29*).

Rhodium binding and oxidation were examined in the promoter region of the phosphoglycerate kinase gene (PGK1), for which the transcription factor binding pattern is well-characterized (Figure 4a) and for which LMPCR primers and protocols are well-established (*24*, *26*, *30*). This region features two GC boxes, containing three consensus binding

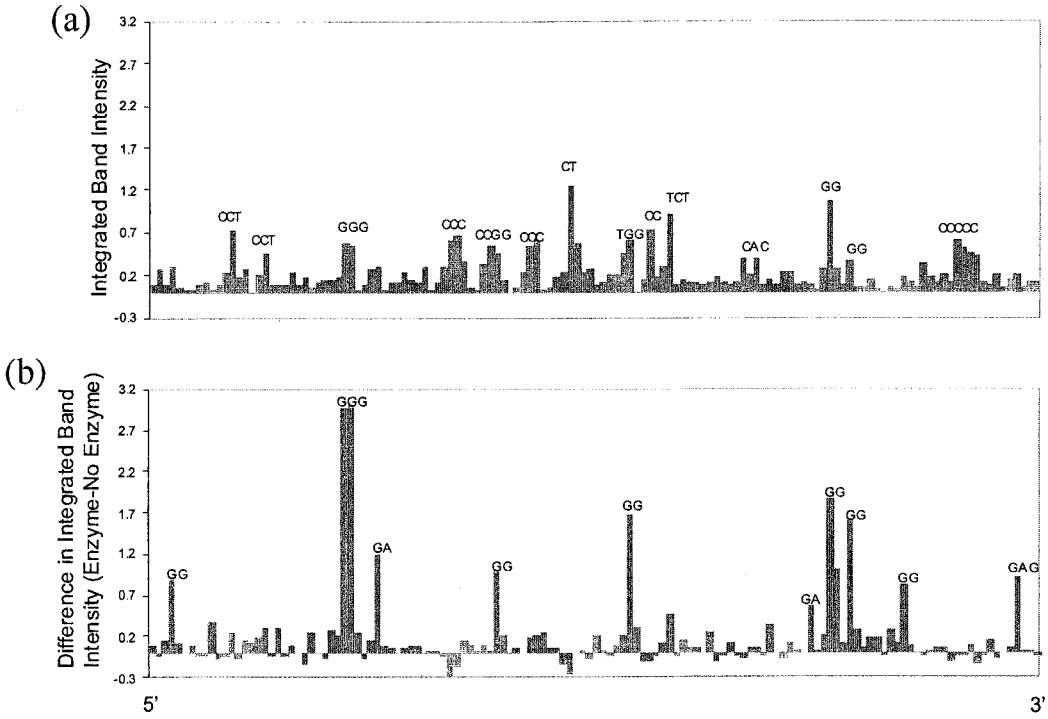

FIGURE 2: DNA damage promoted by photoactivated $Rh(phi)_2DMB^{3+}$ on exon 5 of the p53 gene inside of isolated nuclei. (a) Frank strand breaks corresponding to the rhodium complex binding sites are shown. The complex binds in a fairly sequence-neutral fashion, although it prefers to cleave at the sugars of pyrimidines (*18*, *27*, *28*). Approximately 25 bp are excluded from each end of the exon for clarity on the histogram. (b) The base damage is subsequently revealed by treatment with Fapy glycosylase and EndoIII base excision repair enzymes. The most heavily oxidized site is the sole 5′-GGG-3′ site in this exon, followed by the 5′-GG-3′ and 5′-GA-3′ sites, fully consistent with oxidation by $Rh(phi)_2DMB^{3+}$ from a distance through the DNA π stack.

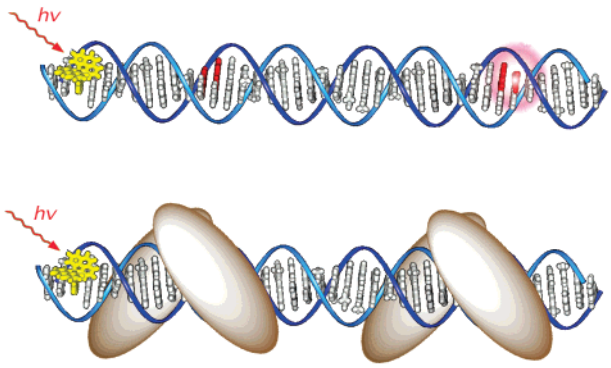

FIGURE 3: Assay for oxidation of guanine from a distance by $Rh(phi)_2DMB^{3+}$ inside isolated nuclei. To determine whether charge transfer can occur at long range on DNA inside of nuclei (top), the oxidation of guanines that are protected from direct access of the rhodium complex was monitored in the presence of stable DNA-binding proteins. Oxidation of these guanine sites must occur from a distance (bottom).

sites for the Sp1 zinc-finger transcription factor, as well as a CCAAT sequence and a region that is reasonably homologous to two transcription factor NF1 binding sites.

A comparison of the pattern and intensity of rhodium-induced frank strand breaks on naked DNA to that on DNA isolated from nuclei reveals clear footprints on the LMPCR sequencing gel. The levels of rhodium binding and direct DNA backbone cleavage are diminished by the proteins bound to this promoter within the nucleus. In the NF1-like region, for example, the intensity of frank strand breaks is decreased noticeably on the transcribed strand, corroborating protein binding at this site (Figure 4b, lanes 2 and 3). On the nontranscribed strand, frank strand breaks by rhodium are rare in the NF1-like region, on both rhodium-treated naked DNA and DNA isolated from nuclei, because this strand is purine-rich. Nevertheless, strong oxidative damage is apparent and is enhanced at the central 5′-GGG-3′ site on the DNA isolated from rhodium-treated nuclei compared to naked DNA (Figure 4c, lane 4).

Results are shown as histograms in Figure 5. Photofootprinting by the rhodium complex is evident when the intensity of frank strand breaks in the rhodium-treated naked DNA is subtracted from that of DNA isolated from rhodium-treated nuclei (Figure 5a). The strong footprint in the NF1-like region is seen clearly (red). Interestingly, this footprint appears to be displaced by a few base pairs relative to that sequence footprinted using DNAse I (*24*), and this shift is consistent with rhodium and DNAse I binding and cleaving by different mechanisms and in different grooves of the helix (*31*). A significant decrease in the level of frank strand breaks in nuclear DNA is seen also in the CCAAT box protein-binding region on both the transcribed strand (Figure 5a) and the nontranscribed strand (not shown). It is noteworthy that frank strand breaks are increased in the region between the NF1-like and CCAAT box regions, indicating that rhodium intercalation is facilitated by binding of transcription factors to the DNA sequences flanking this region. Such a hyperreactivity has been seen previously (*24*, *32*). In the experiment illustrated here, only a weak footprint, at best, is seen at the GC box proximal to the transcriptional start site (Figure 5a, green); other cell preparations have shown more significant footprinting at this site. A strong footprint is also seen for the more distal GC box, but on the complementary strand that contains mostly pyrimidines (data not shown). As with the NF1-like box, in both GC boxes,

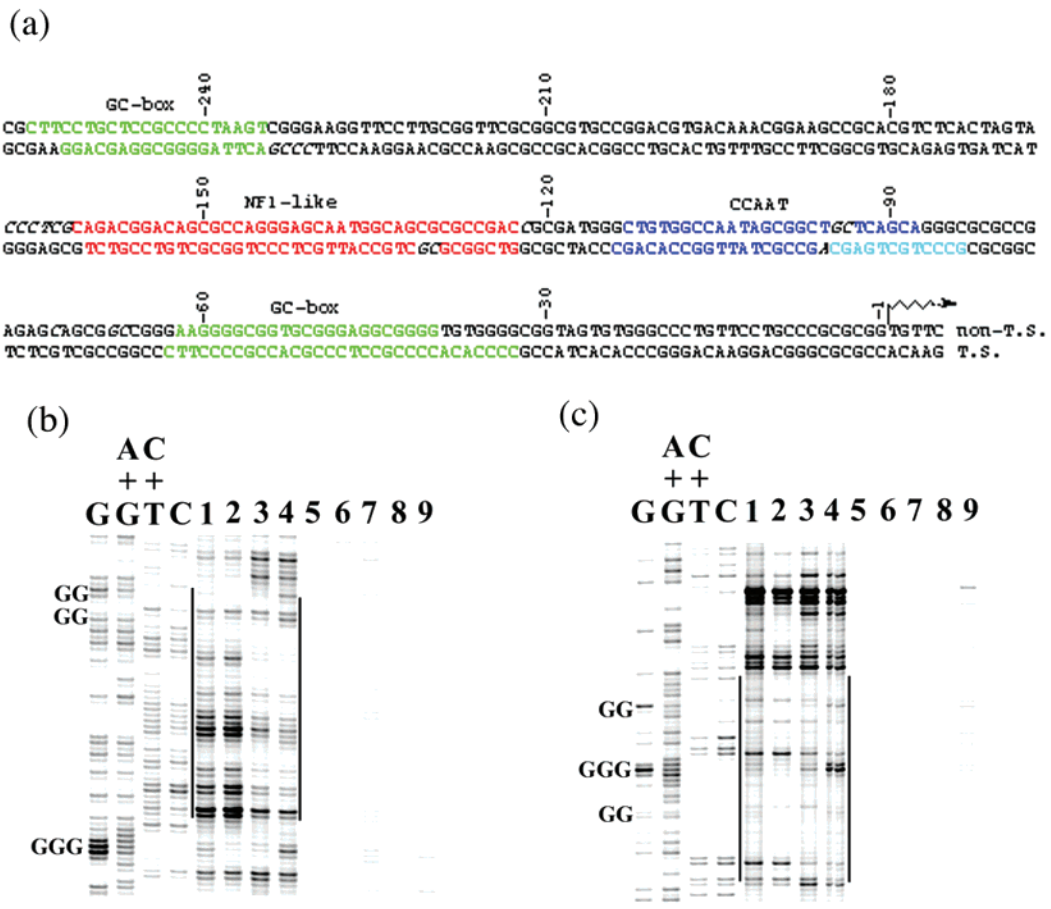

FIGURE 4: Analysis of long-range guanine oxidation on the PGK1 promoter inside nuclei. (a) Sequence of a part of the upstream promoter region of the PGK1 gene, showing regions of the promoter which reproducibly bind transcription factors, as revealed by DNAse I and DMS footprinting followed by LMPCR (*24*, *30*). Red, green, and blue (and, to a lesser degree, cyan) regions showed a decrease in the level of cleavage by DNAse I in vivo, whereas italicized bases flanking the protein binding sites showed increases in the level of cleavage. PGK is an X-linked gene which is constitutively active in normal male cells and in one copy in normal female cells. Although *HeLa* cells are derived from female cells, they contain only active X chromosomes. Any copies of PGK are active and demonstrate transcription factor footprints. (b) LMPCR-amplified DNA cleavage after treatment of bare DNA or nuclei with rhodium and photoactivation is shown for the transcribed strand of the PGK promoter near the NF1-like binding site (residues −113 to −175). The location of the bound protein as determined by DNAse I is indicated by dark bracketed lines. Maxam−Gilbert sequencing lanes are shown at the right. All samples were treated with Fapy glycosylase and EndoIII, unless otherwise indicated: lane 1, naked DNA, without Fapy glycosylase or EndoIII; lane 2, naked DNA; lane 3, nuclei; lane 4, nuclei, without Fapy glycosylase or EndoIII; lane 5, naked DNA without photoirradiation; lane 6, naked DNA without rhodium; lane 7, nuclei without photoirradiation; lane 8, nuclei without rhodium; and lane 9, naked DNA without photoirradiation or rhodium. Note that there is a significant reduction in the level of frank strand breaks between the naked DNA and nuclear DNA samples in the region of the NF1-like box (compare lanes 2 and 3), resulting in a footprint, and an increase in the level of frank strand breaks flanking the NF1-like region toward the top of the gel. (c) LMPCR-amplified DNA cleavage after treatment of bare DNA or nuclei with rhodium and photoactivation is shown for the nontranscribed strand near the NF1-like box (residues −185 to −119): lane 1, naked DNA without Fapy glycosylase or EndoIII; lane 2, naked DNA; lane 3, nuclei; lane 4, nuclei, without Fapy glycosylase or EndoIII; lane 5, naked DNA without rhodium or photoirradiation; lane 6, naked DNA without rhodium; lane 7, nuclear DNA without rhodium; lane 8, naked DNA without photoirradiation; and lane 9, nuclear DNA without photoirradiation. Note that although there are very few frank strand breaks in either the nuclear or naked DNA on this strand by which to establish protein binding (lanes 2 and 3), there is a strong enzyme-dependent band in the nuclear DNA lanes at the location of a 5′-GGG-3′ site (lane 4).

frank strand breaks are seen preferentially on the cytosine-rich strand, which is characteristic of the rhodium complex.

Importantly, despite the fact that rhodium binding is inhibited by transcription factors, significant oxidative base damage is still apparent. As seen earlier on the p53 exon, the base damage revealed by treatment with Fapy glycosylase and EndoIII occurs at guanine multiplets (Figure 5b). This 5′-GG-3′ and 5′-GGG-3′ specific damage is fully consistent with a charge transport mechanism for DNA damage in this region. Furthermore, the pattern of frank strand breaks indicates that rhodium binding is not uniformly distributed over the PGK promoter, but guanine multiplets are damaged at sites footprinted for NF1, CCAAT, and the proximal GC box. Guanine multiplets are also preferentially damaged in the distal GC box on the complementary strand (not shown).

A plot of intensity of all guanine damage in nuclear DNA expressed as a percentage of damage versus that on the naked DNA can be used to compare directly the level of damage obtained within the nuclei versus that for DNA in the absence of bound protein (Figure 5c). Damage to guanine multiplets is enhanced in nuclei relative to naked DNA, but the small extent of damage at most of the single guanine sites in nuclei is modestly diminished, especially in regions which are proposed to bind proteins. Within the NF1-like protein binding region, there is a small decrease in the level of

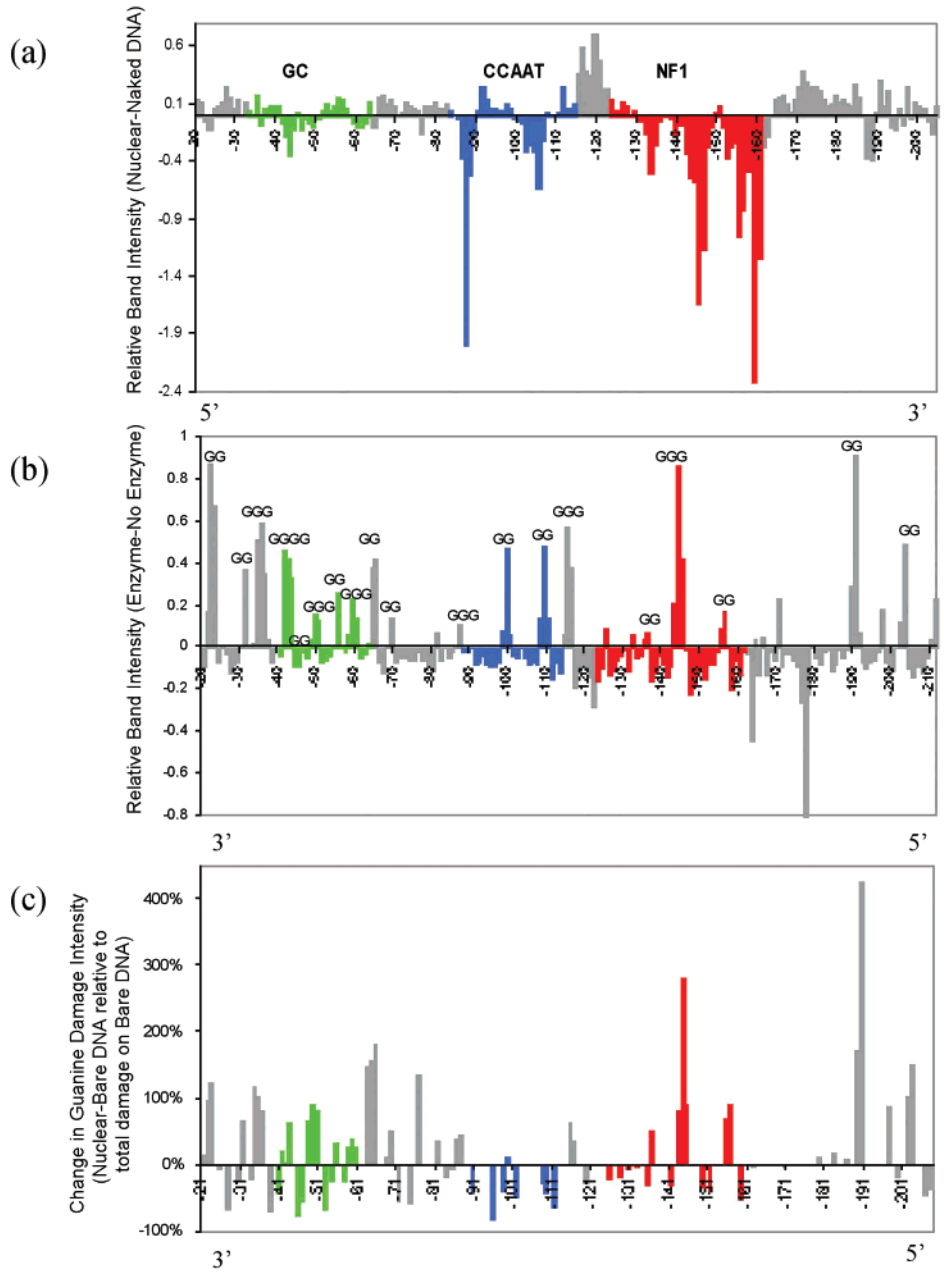

FIGURE 5: Binding and base damage by a rhodium metallointercalator in the PGK promoter region. (a) Difference between the frank strand breaks on the nuclear DNA and the naked DNA (transcribed strand). Colored regions correspond to the protein-binding domains (Figure 4a). This difference histogram illustrates footprints in the transcribed strand at the CCAAT and NF1-like sequences and a "positive footprint" of increased sensitivity to rhodium binding and/or cleavage between the two proteins. (b) Base damage in nuclear DNA as revealed by treatment with Fapy glycosylase and EndoIII (nontranscribed strand). Guanine bases are preferentially oxidized, as in the p53 gene, and no footprints are apparent at the protein binding sites. (c) Plot of the intensity of all guanine damage in nuclear DNA expressed as a percentage of damage vs that on the bare DNA (nontranscribed strand), comparing directly the level of damage obtained within the nuclei vs that for DNA in the absence of bound protein. Damage to 5′-guanines in guanine multiplets is better in nuclei than in naked DNA, but the small extent of damage at most of the single guanine sites and 3′-guanines in nuclei is modestly diminished, especially in regions which are proposed to bind proteins. Since there appears to be no significant diminution in the level of oxidation at protein binding sites, it appears that sites that are blocked from direct binding of the rhodium complex can be oxidatively damaged from a distance. Note that although both frank strand breaks at guanine and oxidative guanine base damage are represented in this histograms, the majority of the cleavage events are due to the latter reaction, especially at multiple guanine sites, due to the inherent sequence preferences of the two rhodium photoreactions.

damage at single guanine sites, consistent with reduced rhodium binding and frank strand breaks in this region, but an increase in the level of damage at the two 5′-GG-3′ sites and a 300% increase in the level of damage at the 5′-GGG-3′ site. The strong oxidation at the 5′-GGG-3′ site in the middle of this NF1-like binding sequence can also be seen clearly on the gel (Figure 4c). This enhancement in long-range oxidative damage with protein binding has been seen in studies of long-range charge transport in the presence of DNA-bound proteins having the helix−turn−helix motif (*29*). Such enhancements may be due to the effects of increased rigidity in stacking on charge transport, or to changes in the trapping time of a radical intermediate.

Guanine damage within the CCAAT box and the proximal GC box also shows, in general, an increase in the number of 5′-guanines of guanine multiplets but a decrease in the

level of damage at 3′-guanines or single guanines. Clearly, then, there is no significant diminution in the level of oxidation across this promoter despite the presence of bound proteins. These data indicate that sites that are blocked from direct binding of the rhodium complex are nonetheless able to be oxidatively damaged. *Guanine oxidation therefore must occur through the DNA π stack from a distance*.

The distances over which this charge transport occurs cannot be established with certainty, given the many sites that are available to the rhodium complex. Nonetheless, the protein footprints are sufficiently large to conclude that guanine oxidation occurs from a distance of at least 5 or 10 bp (17−34 Å) and possibly from as far as ≥30 (100 Å). The upper distance limits of charge migration within the cell remain to be determined.

Implications. Charge transport through DNA to effect oxidative damage at a distance has become well-established (*2*−*16*). The data presented here extend DNA charge transport as a feasible mechanism for the generation of DNA base lesions within the cellular environment. DNA inside of cells is therefore susceptible to damage that arises from a remotely bound site, indeed even at sites that are inaccessible directly as a result of protein binding. It will be worthwhile to examine mutagens and therapeutic natural products that are known to generate base radicals to determine if they operate through a similar mechanism (*33*, *34*). It will also be important to determine whether organisms have evolved to protect their genomes from long-range damage. Perhaps radical damage is funneled to or insulated from specific sites within the genome. We do not suggest on the basis of these data that radical migration occurs over megabase distances, and indeed, studies on DNA restriction fragments would suggest that charge transport over those distances is not likely (*12*). One could, however, consider that segments throughout the genome may encode "sinks" for damage, and that other segments could serve as buffers as a result of local sequence-dependent or protein-dependent structural deformations to protect critical regions. Certainly, the biological consequences and opportunities for DNA-mediated charge transport now require consideration.

ACKNOWLEDGMENT

We thank Ning Ye, Shu-mei Dai, and Steven Bates for their technical assistance, Timothy O'Connor for the Fapy/EndoIII enzyme mixture, and Daniel Hall and Katherine Noyes for their help with the synthesis of $Rh(phi)_2DMB^{3+}$.

REFERENCES

1. Friedberg, E. C., Walker, G. C., and Siede, W. (1995) *DNA Repair and Mutagenesis*, American Society for Microbiology Press, Washington, DC.
2. Kelley, S. O., and Barton, J. K. (1998) in *Metal Ions in Biological Systems* (Sigel, A., and Sigel, H., Eds.) pp 211−249, Marcel Dekker, New York.
3. Núñez, M. E., and Barton, J. K. (2000) *Curr. Opin. Chem. Biol. 4*, 199.
4. Hall, D. B., Holmlin, R. E., and Barton, J. K. (1996) *Nature 382*, 731.
5. Gasper, S. M., and Schuster, G. B. (1997) *J. Am. Chem. Soc. 119*, 12762.
6. Núñez, M. E., Hall, D. B., and Barton, J. K. (1999) *Chem. Biol. 6*, 85.
7. Henderson, P. T., Jones, D., Hampikian, G., Kan, Y., and Schuster, G. B. (1999) *Proc. Natl. Acad. Sci. U.S.A. 96*, 8353.
8. Hall, D. B., and Barton, J. K. (1997) *J. Am. Chem. Soc. 119*, 5045.
9. Rajski, S. R., Kumar, S., Roberts, R. J., and Barton, J. K. (1999) *J. Am. Chem. Soc. 121*, 5615.
10. Boon, E. M., Ceres, D. M., Drummond, T. G., Hill, M. G., and Barton, J. K. (2000) *Nat. Biotechnol. 18*, 1096.
11. Saito, I., Takayama, M., Sugiyama, H., and Nakatani, K. (1995) *J. Am. Chem. Soc. 117*, 6406.
12. Núñez, M. E., Noyes, K. T., Gianolio, D. A., McLaughlin, L. W., and Barton, J. K. (2000) *Biochemistry 39*, 6190.
13. Arkin, M. R., Stemp, E. D. A., Coates Pulver, S., and Barton, J. K. (1997) *Chem. Biol. 4*, 389.
14. Hall, D. B., Kelley, S. O., and Barton, J. K. (1998) *Biochemistry 37*, 15933.
15. Schuster, G. B. (2000) *Acc. Chem. Res. 33*, 253.
16. Giese, B. (2000) *Acc. Chem. Res. 33*, 631.
17. Kielkopf, C. L., Erkkila, K. E., Hudson, B. P., Barton, J. K., and Rees, D. C. (2000) *Nat. Struct. Biol. 7*, 117.
18. Sitlani, A., Long, E. C., Pyle, A. M., and Barton, J. K. (1992) *J. Am. Chem. Soc. 114*, 2303.
19. Burrows, C. J., and Muller, J. G. (1998) *Chem. Rev. 98*, 1109.
20. Steenken, S., and Jovanovic, S. V. (1997) *J. Am. Chem. Soc. 119*, 617.
21. Sugiyama, H., and Saito, I. (1996) *J. Am. Chem. Soc. 118*, 7063.
22. Prat, F., Houk, K. N., and Foote, C. S. (1998) *J. Am. Chem. Soc. 120*, 845.
23. Pfeifer, G. P., Drouin, R., and Holmquist, G. P. (1993) *Mutat. Res. 288*, 39.
24. Pfeifer, G. P., and Riggs, A. D. (1991) *Genes Dev. 5*, 1102.
25. Drouin, R., Rodriguez, H., Holmquist, G. P., and Akman, S. A. (1996) in *Technologies for Detection of DNA Damage and Mutations* (Pfeifer, G., Ed.) pp 211−225, Plenum Press, New York.
26. Dai, S.-M., Chen, H.-H., Chang, C., Riggs, A. D., and Flanagan, S. D. (2000) *Nat. Biotechnol. 18*, 1108.
27. Sitlani, A., and Barton, J. K. (1994) *Biochemistry 33*, 12100.
28. Uchida, K., Pyle, A. M., Morii, T., and Barton, J. K. (1989) *Nucleic Acids Res. 17*, 10259.
29. Rajski, S. R., and Barton, J. K. (2001) *Biochemistry 40*, 5556.
30. Pfeifer, G. P., Tanguay, R. L., Steigerwald, S. D., and Riggs, A. D. (1990) *Genes Dev. 4*, 1277.
31. Tullius, T. D. (1989) *Annu. Rev. Biophys. Biophys. Chem. 18*, 213.
32. Dervan, P. B. (1986) *Science 232*, 464.
33. Rodriguez, H., Holmquist, G. P., D'Agostino, R., Jr., Keller, J., and Akman, S. A. (1997) *Cancer Res. 57*, 2394.
34. Rodriguez, H., Drouin, R., Holmquist, G. P., O'Connor, T. R., Boiteux, S., Laval, J., Doroshow, J. H., and Akman, S. A. (1995) *J. Biol. Chem. 270*, 17633.

BI011560T